

# Building a Performance Model for Deep Learning Recommendation Model Training on GPUs

1<sup>st</sup> Zhongyi Lin  
ECE Department  
University of California, Davis  
Davis, California  
zhylin@ucdavis.edu

2<sup>nd</sup> Louis Feng  
Facebook, Inc  
Menlo Park, California  
lofe@fb.com

3<sup>rd</sup> Ehsan K. Ardestani  
Facebook, Inc  
Menlo Park, California  
ehsanardestani@fb.com

4<sup>th</sup> Jaewon Lee  
Facebook, Inc  
Menlo Park, California  
jaewon@fb.com

5<sup>th</sup> John Lundell  
Facebook, Inc  
Menlo Park, California  
jlundell@fb.com

6<sup>th</sup> Changkyu Kim  
Facebook, Inc  
Menlo Park, California  
ckkim@fb.com

7<sup>th</sup> Arun Kejariwal  
Facebook, Inc  
Menlo Park, California  
akejariwal@fb.com

8<sup>th</sup> John D. Owens  
ECE Department  
University of California, Davis  
Davis, California  
jowens@ucdavis.edu

**Abstract**—We devise a performance model for GPU training of Deep Learning Recommendation Models (DLRM), whose GPU utilization is low compared to other well-optimized CV and NLP models. We show that both the device active time (the sum of kernel runtimes) and the device idle time are important components of the overall device time. We therefore tackle them separately by (1) flexibly adopting heuristic-based and ML-based kernel performance models for operators that dominate the device active time, and (2) categorizing operator overheads into five types to determine quantitatively their contribution to the device active time. Combining these two parts, we propose a critical-path-based algorithm to predict the per-batch training time of DLRM by traversing its execution graph. We achieve less than 10% geometric mean average error (GMAE) in all kernel performance modeling, and 5.23% and 7.96% geomean errors for GPU active time and overall end-to-end per-batch training time prediction, respectively. We show that our general performance model not only achieves low prediction error on DLRM, which has highly customized configurations and is dominated by multiple factors, but also yields comparable accuracy on other compute-bound ML models targeted by most previous methods. Using this performance model and graph-level data and task dependency analyses, we show our system can provide more general model-system co-design than previous methods.

**Index Terms**—DLRM, GPU, performance modeling, machine learning.

## I. INTRODUCTION

Recommendation models (RMs) have been widely deployed across various industries to improve user experiences and engagements in products and services. Examples include search [1], shopping [2], media consumption [3], [4], and social networking [5]. Driven by ever-increasing demands, training these models for better prediction rates has become both data- and computationally intensive: the training data volume can be hundreds of billions of examples, and the model sizes range from a few hundred GBs to multiple TBs [6]. Large RMs require distributed training on multiple (often hundreds of) hosts and devices [7].

Such models incur high resource demands for development, debugging, and optimization, which significantly affects the

productivity of ML engineers and operation cost of data centers. Therefore, a performance model that accurately predicts an RM’s training performance (e.g., speed, memory usage, etc.) based on its configurations (e.g., batch size, data sharding, number of layers, etc.) is very useful. It removes dependencies on hardware for some tasks and relieves these resource burdens. The flexibility to get performance metrics for varying inputs and configurations helps researchers answer what-if questions, identify bottlenecks, and better meet design constraints. Performance models can help answer questions like:

- How does changing batch size and/or number of parameters impact performance and memory constraints?
- How much performance gain can be achieved with new GPUs?
- Can operator (op) fusion or other optimizations improve performance?
- How to improve embedding table sharding load imbalance?

Our performance model can provide high-confidence metrics to answer these and other questions without the need to profile the workload on GPUs. Insights into the RM workload characterization also provide opportunities for model-system co-design. However, building such a performance model faces three major challenges:

- Models with lower GPU utilization are difficult to model. We quantify “GPU utilization” as the percentage of *per-batch training time* when kernels are running on the device.<sup>1</sup> Some vision (CV) and natural language processing (NLP) models like ResNet [10] and Transformer [11] have high GPU utilization (Figure 1). We can accurately model end-to-end runtime in these models by simply adding their constituent kernel runtimes. However, in this paper, we focus on low-GPU-utilization recommendation models. As an example, perhaps the most impactful RM is DLRM [8],

<sup>1</sup>This is slightly different from *nvidia-smi*’s definition of GPU utilization, which is measured over a sample period between 1 and 1/6 second.

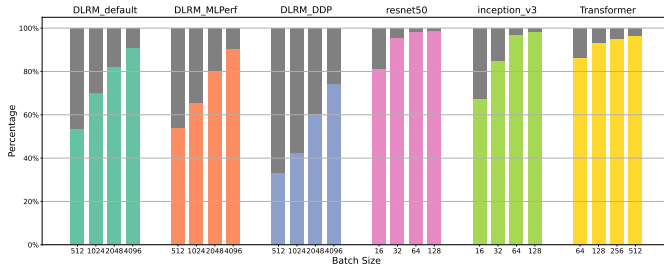


Fig. 1. GPU utilization of per-batch training time of six DL models on a NVIDIA Tesla V100 GPU. Batch sizes shown here are those commonly used in training. Recommendation models (*DLRM\**) have substantially more device idle time than other models. Whereas other models can be adequately modeled by summing kernel time, modeling RMs is a more complex problem.

open-sourced by Facebook in 2019 and currently one of the reference implementation models in MLPerf [9]. DLRM has significantly lower GPU utilization than other DL models (Figure 1). We thus cannot accurately model DLRM, or other low-GPU-utilization models, with the simpler techniques used for high-GPU-utilization models.

- The combination of GPU asynchronous execution with task and data dependencies makes it difficult to estimate the contribution of each operator’s device kernel time and host-side overhead to the per-batch training time on the device. Also, resulting host-side overheads may result in an idle GPU. Previous approaches focused on op-level execution times did not account for these complexities, missing opportunities for a more general and accurate approach.
- Finally, an RM comprises a broader range of operators (“ops”) than convolution-dominated CNNs and matrix-multiply-dominated Transformers. While simple models with one kernel performance model may suffice for these simpler cases, RMs require more kernel performance models to characterize their behavior.

In summary, previous performance models for DL workloads were not accurate enough to model DLRM and by extension other complex workloads because they did not address low-GPU-utilization, asynchronous, or many-complex-operator workloads. Our research addresses these complexities by proposing a new performance model for the GPU training of DLRM. Here, we focus on a single-GPU configuration, leaving multi-GPU for future work. We begin by analyzing the device execution time of DLRM to identify dominating operators and kernels. Then, using heuristic or ML approaches, we build performance models for these kernels for a wide range of input configurations. Using our runtime observer inside PyTorch, we record DLRM’s execution graph for its inputs, outputs, and data dependencies. Combining the above components and the ML model execution graph, we construct a critical-path-based end-to-end performance model for DLRM training on GPUs. This method achieved 5.23% and 7.96% geomean errors for per-batch GPU active time and training latency, respectively, compared to actual measured time collected by running the DLRM benchmark.

Our overall performance model relies on accurate kernel

models. The kernel models we built achieve less than 10% geometric mean average error (GMAE) in predicting kernel execution time. The principles and techniques we used to model kernels can model other kernels that are not included in DLRM as well. Beyond an accurate kernel model, we also must incorporate host-side overheads into our model. This analysis is a key insight of our work. We categorize host-side overheads into five types and show, based on many measurements, that these overheads are consistent across different ops.

We compared our performance model with several existing performance models on representative CV and NLP models beyond DLRM. The results show that our method is general and works well across a variety of workloads on different generations of GPUs. We discuss one potential use case of our performance model at the end of the paper: assisting practical model-system co-design with the support of the execution graph. Our contributions in this research include:

- For predicting GPU training time of DL models, we show our critical-path-based end-to-end performance model is a more generalized solution than methods that only focus on the device active time, especially those with low GPU utilization such as DLRM.
- Compared to op-based methods, we separately predict kernel time and GPU idle time and show this separation facilitates performance modeling by sharing kernel performance models across ops that call the same type of kernels and thus reducing the cost of collecting metrics from microbenchmarks.
- With our specialized model execution graph observer that captures data dependencies among ops, we provide more flexible simulation and performance modeling options that together assist model-system co-design. Users can predict their optimization of DL models by simply transforming and changing the model execution graph without actually running the computation on GPUs. In particular, using these captured data dependencies between ops, we can model performance impacts from changing batch size, hardware, operator fusion, reordering, and parallelization that previous methods cannot do.

## II. RELATED WORK

### A. GPU operator and kernel performance models

Op-level and kernel-level performance models usually fall into two categories. *Heuristic models* (e.g., the roofline model [12]) estimate the kernel execution time by estimating memory traffic, floating point operations, etc. *ML-based models* are trained with benchmark data of kernel execution to predict kernel time for any input size. Heuristic models, except for those for trivial (e.g., element-wise) ops/kernels, require the source code to be accessible, while ML-based models require a benchmark dataset of reasonable size. While training with this benchmark dataset may take a long time, the training is a one-time cost per device.

a) *Models for GEMM-based kernels:* With the current PyTorch release, MLP layers in DLRM rely on cuBLAS and

its GEMM-based kernels as the low-level implementation on NVIDIA GPUs. Either using the roofline model or designing a heuristic performance model for these kernels turns out to be infeasible because of not only the lack of source code, but also the special tile quantization and wave quantization effects of cuBLAS [13]. In existing research (e.g., Lym et al. [14]) on heuristic performance model design for proprietary libraries like cuDNN, many parameters are still opaque or extremely difficult to measure. Therefore, rather than heuristic ones, an ML-based performance model is more suitable in this case. Previous work [15], [16] shows that either a CNN or MLP model is sufficient to capture the performance features of the GEMM operation. In our work, we use MLP to construct the performance model for cuBLAS kernels called by PyTorch ops like *addmm*, *bmm*, *linear*, etc., which are all GEMM-based.

### B. Model-level performance modeling

Previous work [15]–[19] mainly focuses on CNNs and/or NLP models, which, as we noted above, are primarily dominated by compute-bound convolution ops and have high GPU utilization. Our work, in contrast, not only targets a more complex model (DLRM) that can be highly customized and thus may be dominated by compute, memory operations, or communication, but also handles DLRM’s substantial device idle time in our end-to-end training time prediction. *Daydream* [20] predicts model runtime after certain optimizations by simulating execution based on the kernel-task dependency graph. This work has a similar approach to ours in addressing the timing of both CPU and GPU threads; however, it lacks the ability to directly predict individual kernel runtime. This limits its capability in predictions for varying input and configuration changes without recollecting performance data using hardware. Separately, *Habitat* [16] presented a performance predictor using MLP models trained with kernel metrics. It showed that combining *Habitat* and *Daydream* resulted in a higher average error of 16.1% than *Daydream* alone. We reduce prediction error compared to this previous work by actually predicting the kernel runtime and overheads based on a finer granularity of instrumentation. In addition, *Daydream*’s kernel dependency graph does not capture data dependencies and thus is limited in discovering and predicting the efficacy of other optimizations such as concurrent kernel execution. In our work, data dependencies are well-captured by the execution graph and therefore we can accurately model a wider variety of optimizations, such as performance-model co-design. Table I summarizes different features implemented in previous work and ours. To the best of our knowledge, our work is the first that can successfully target the performance modeling complexities characteristic of complex models like DLRM.

### C. Recommendation Models and DLRM

RMs have evolved from collaborative filtering [21], neighborhood methods [22], and simple regression-based predictive models [23] to deep-learning-based RMs [8], [24]–[27]. Some deep learning models also consider sequences of users’ actions. For example, the Deep Interest Evolution Network (DIEN) uses

TABLE I. Comparison of our work with previous ones. Abbreviation examples: **J** (Justus et al. [17]), **P** (Pei et al. [18]), **L** (Liao et al. [15]), **Z** (Zhu et al. [20]), **Y** (Yu et al. [16]). End-to-end prediction of Zhu et al. is marked as ‘Limited’ since it only estimates the efficacy of optimization on certain kernels instead of making prediction for every single kernel.

Work	Kernel Pred.	Idle Time Pred.	E2E Pred.	Target Model Types
J [17]	✓	✗	✓	CNNs
P [18]	✓	✗	✓	CNNs
L [15]	✓	✗	✓	CNNs
Z [20]	✗	✗	Limited	Multiple
Y [16]	✓	✗	✓	Multiple
Ours	✓	✓	✓	Multiple + RMs

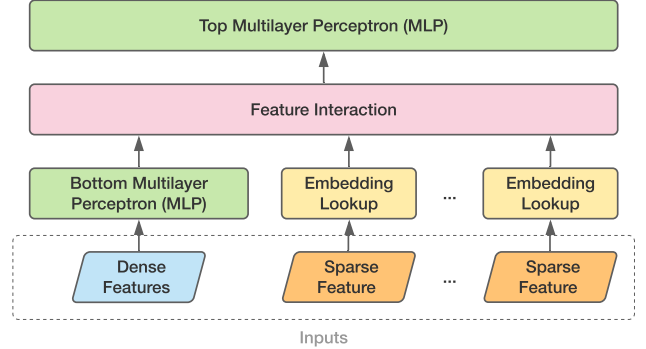


Fig. 2. The high-level model architecture of DLRM. The inputs (usually user and product data in practice) can be dense and sparse (categorical) features. Each embedding table contains up to millions of embedding vector and hundreds of values per vector, and because of which they are often sharded across multiple devices in the distributed training.

GRU layers to model temporal user behaviors [28]. The key characteristics that differentiate RMs from CNNs and NLPs are a mixture of sparse and dense computations, large training data volumes, and large, potentially unbounded model sizes.

We choose to use DLRM implemented in PyTorch as a modern representative workload in our analysis. Figure 2 depicts DLRM’s high-level model architecture. In contrast to embedding table lookups, which are memory-intensive, the multilayer perceptron (MLP) operations are compute-intensive, while any or both of them can dominate the execution time. Besides, the feature interaction is bounded by communication if the model is trained on a multi-GPU platform, and the inputs might be memory-capacity-bound if the training data size is large. Compared to other kinds of models, including CNNs and NLPs, DLRM are potentially bounded by these multiple factors, and as a result building a performance model for it is technically more challenging.

## III. METHODOLOGY

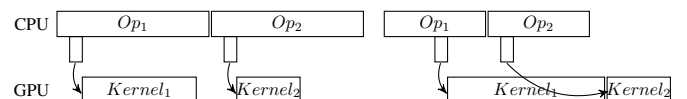


Fig. 3. Two cases for dependent ops. The small rectangles below the (CPU) ops indicate the launch of their GPU kernels. The left trace is CPU-bound and the right one is GPU-bound. In either case, summing the device active time of the two ops does not properly represent the total execution time, in part because host-side overheads are not considered.

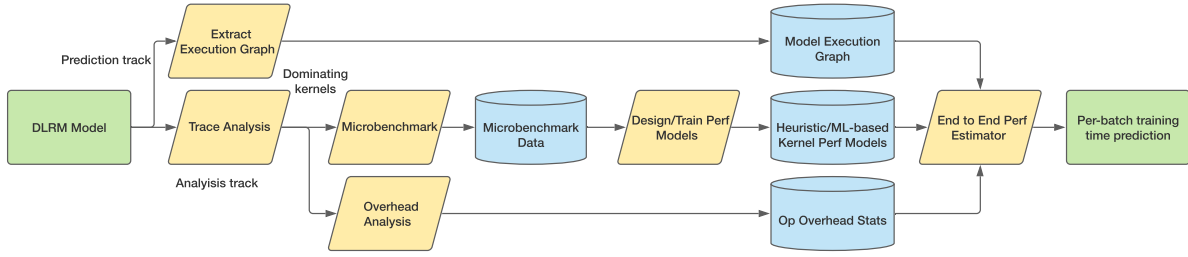


Fig. 4. An overview of our prediction pipeline. We begin with DLRM models taken as inputs. These are sent through the *Analysis Track* for trace analysis, microbenchmark data collection, kernel performance model design/training, and op overhead analysis. Armed with these analyses, subsequent DLRM models simply go through the *Prediction Track*, where their execution graphs are extracted and their performance is predicted. This prediction pipeline is designed to be a modular system, so that building blocks of the pipeline marked with blue cylinders can be reused and enriched.

Typically, the per-batch training time is estimated by summing the execution time of each *op* in a certain way. Op execution time can be either measured at the host or the device as the sum of kernel execution time. Since GPU kernels are scheduled asynchronously, it is hard to accurately predict an op’s *host time* from the computation it conducts, and thus the op’s execution on the device is usually the time to be measured. For example, CNNs usually resemble the right-hand-side case in Figure 3: ops are mostly convolution and GPU compute-bound, and therefore they usually have high GPU utilization. Previous studies that have primarily targeted CNNs can safely make the prediction by summing the individual kernel time and the effects of omitting CPU overheads are minimal. However, this method is sometimes not sufficient to accurately model the end-to-end execution time, if the model’s GPU utilization is low. As we show previously in Section I, DLRM, with their varying sizes and composition of ops, could possibly resemble either the left or right cases in Figure 3 and have as low as 40% GPU utilization. This means that the per-batch training time prediction error will be 60% by following the same method, even if the kernel prediction accuracy is 100%. The cause of low GPU utilization varies. Some are because of inefficiencies, while others are constrained by the inherent model design. These complexities necessitate a better methodology of building the performance model for DLRM as well as other models with low GPU utilization.

To address this challenge, we devise a performance modeling pipeline that separates the prediction of device active time and idle time, and integrates both parts with a critical-path-based algorithm that tracks the execution time on both the CPU and GPU. Such a separation brings two major advantages in building kernel performance models:

- Ops (e.g., *addmm/bmm* vs. *AddmmBackward* vs. *BmmBackward*) that have the same type of kernel calls (i.e., cuBLAS GEMM kernels) can share the same performance model. This saves us a large amount of time for microbenchmarking and training of ML-based kernel performance models.
- Although ML-based performance models can predict kernel time and op overheads as a whole for each op, heuristic models solely based on an op’s mathematical expression are not able to address its overheads. Separating them allows us to flexibly choose between the approaches

of heuristic and ML-based models, while the overheads are handled separately.

Figure 4 depicts an overview of the prediction pipeline. The remainder of this section explains how each building block of the pipeline works in detail.

#### A. Per-batch Training Time Breakdown

To understand the device active time and identify dominating ops and kernels, we perform a breakdown of per-batch training time through analyzing PyTorch profiler trace files, in which the metadata of all events, i.e., calls to operators, is flattened. We construct an event tree to keep track of the calling stack of each op so that the device execution time of each kernel is attributed to the corresponding op, and thus we know the dominating kernels by knowing the dominating ops. We present the device time breakdown of three DLRM models (configurations shown later) in Figure 5 and the kernel breakdown of its dominating ops in Figure 6. We again observe that the device-side idle time forms a non-negligible proportion of the total device time, because the host-side op overheads and data dependencies implicitly contribute to it by blocking the scheduling of GPU kernels. This result motivates the necessity of our proposal of analyzing the kernel execution time and overheads separately.

As we noted in Section I, ops in RMs are complex. We observe that there is no single op that dominates the device active time of the model. A list of ops that jointly dominate covers compute-bound ops *addmm* and *bmm*, memory-bound ops (*embedding lookup*), and communication-bound ops *concat* and *to* (memory copy), as well as their counterparts in the backward pass. In this particular case, dense computation (bottom and top MLP) takes almost 70% of the entire device active time, while embedding lookups that might very often dominate in other models is less important. Notice that trivial/element-wise ops such as *relu* and *MseLoss* sum up to around 5% of the end-to-end time. This means they should not be omitted in order to achieve high prediction accuracy. The analysis of the dominating ops’ kernel composition reveals that most of them are composed of or dominated by one single kernel. Exceptions include *AddmmBackward* and *BmmBackward0* that are dominated by two GEMM kernels, and *Optimizer*’s forward and backward ops that are both dominated by a series of element-wise kernels. Ops in the last category are handled by predicting their sum of kernel time as a whole, possibly ignoring minor kernels that do not appreciably impact the



run time. We conclude that there are six major kernels that dominate the per-batch device active time for DLRM training: sparse embedding lookup kernels (both forward/backward) for embedding table lookup, GEMM kernels for bottom and top MLP, and four memory kernels including concatenation, data copy, tensor permutation, and *IndexBackward* (low triangular matrix extraction and flatten in feature interaction).

### B. Microbenchmark and Performance Models for Dominating Kernels in DLRM

We create a benchmark for a total number of seven kernels based on the results we get from the breakdown: the six mentioned above plus the trivial *IndexForward* that partners with *IndexBackward*. The data of this microbenchmark will be used to train and verify the kernel performance models later. Specifically, since all GEMM-related ops are dominated by one or two GEMM kernel calls, it is not necessary to benchmark for all of these ops and we can share the GEMM kernel benchmark data for their performance modeling. We also discover that the only one type of tensor permutations that occurs in DLRM is the batched matrix transpose, i.e., permutation of the second and third axes of a 3D tensor, and thus it becomes the only type of permutation we benchmark. We first execute the corresponding PyTorch operators on one single GPU for 5 iterations as warm-up, then use NVIDIA’s *nvprof* profiler to extract the name of the dominating kernels, and then solely benchmark these kernels for 30 iterations to extract their execution time. Default GPU application clocks are applied, and the CPUs’ turbo boost is turned off, both to guarantee the accuracy and stability of the benchmark.

With this data, we are able to develop kernel performance models for each of the dominating kernels, as it is impossible to apply one single such model to accurately predict the kernel execution time for all dominating kernels we identify. These performance models are designed in two different ways:

- 1) For kernels without *source code access*, such as cuBLAS, PyTorch JIT generated kernels, etc., we predict their execution time with ML-based performance models trained and verified with microbenchmark data.

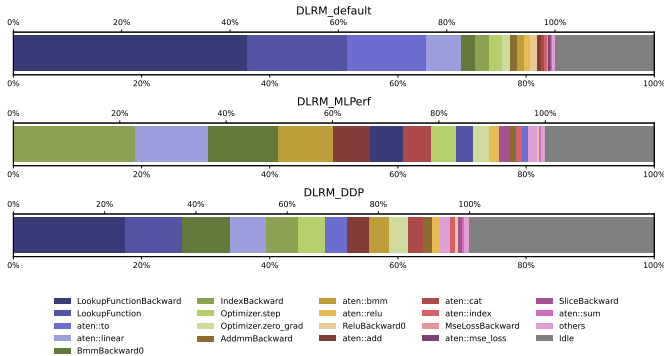


Fig. 5. Device time breakdown of three DLRM models with a batch-size of 2048 on a V100 GPU, with profiler overheads *excluded*. Notice that with different configurations, DLRM is dominated by different kernels, e.g., embedding lookup forward and backward dominates the first and third cases, whereas in the second case it appears to be less important, giving the domination in to *IndexBackward* and FC.

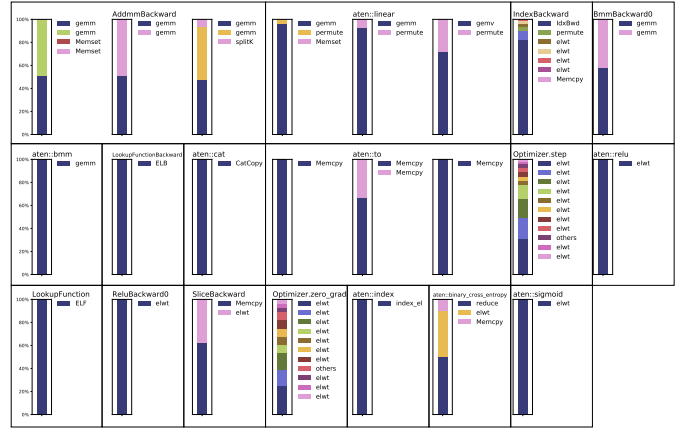


Fig. 6. Kernel composition of dominating ops of *DLRM\_MLPerf*, ordered by their overall execution time. GEMM, ELB, ELF, and memcopy are some of the most important kernels. Abbreviations: *ELF*: embedding lookup forward, *ELB*: embedding lookup backward; *elwt*: element-wise kernel; *gemm/gemv*: cuBLAS internal kernels of any GPU architecture, e.g., Volta, Maxwell, etc.

- 2) For kernels that are either *accessible* or *trivial*, i.e., element-wise, we predict their execution time by either using the roofline model or designing heuristic performance models with memory and throughput estimation through code analysis. As such, the microbenchmark data is solely used to verify the prediction accuracy.

The following subsections explain how these kernel performance models are developed in detail. Our performance models are highly extensible, as the principles and techniques we introduce (code analysis, ML-based kernel performance model training, etc) also apply to any new ops that are not covered by this work.

1) *Characterizing the Embedding Lookup Kernels*: The embedding lookup layers are intrinsically SpMM operations that map categorical features to dense representations. Therefore, the procedure that we describe here for modeling embedding lookup kernels also apply to other kernels of a similar type with irregular memory access patterns and/or is possibly bound by GPU global memory bandwidth. Given a matrix of vector of weights  $A \in \mathbb{R}^{m \times t}$  that contains  $t$  multi-hot vectors of length  $m$  and an embedding table (weight matrix)  $W \in \mathbb{R}^{E \times d}$ , the embedding lookup operation can be written as  $S = A^T W$ . Since a real industrial-scale DLRM model usually contains multiple embedding tables, we can simply concatenate these embedding tables, and pack and batch the input indices into new input tensors, such that the embedding lookup operation over multiple embedding tables can be done in one pass. We integrate the implementation of this batched embedding table lookup algorithm (with SGD for the backward case) from Tulloch [29] into DLRM. Important parameters of the implementation include  $B$  as the batch size,  $E$  as the number of embeddings per table,  $T$  as the number of tables,  $L$  as the number of lookup operations to produce one dense vector, and  $D$  as the embedding vector length. Note that we extend the definition of “warp” for simplicity and refer to a group of threads that all have the same *blockIdx.x/y/z* and *threadIdx.y/z* as a WARP. In practice, this typically refers to

groups of threads of sizes 32, 64, or 128.

We spot that the bounding factor of this op is the memory traffic caused by looking up embedding vectors from the weight tensor. In practice, the value of  $E$  can range from a few hundreds to thousands of millions, while  $L$  is much smaller, i.e., up to one hundred. We can expect that embedding vectors are more frequently fetched from DRAM than from L2 cache. Therefore, we approximate the execution time of the forward kernel by its DRAM access time, which is given by

$$\begin{aligned}
tr\_table\_offsets_w &= 32 \text{ bytes} \\
tr\_offsets_w &= 64 \text{ bytes} \\
tr\_indices_w &= \lceil 4 \times L/32 \rceil \times 32 \text{ bytes} \\
tr\_weights_w &= \lceil 4 \times D/32 \rceil \times 32 \text{ bytes} \\
tr\_outputs_w &= \lceil 4 \times D/32 \rceil \times 32 \text{ bytes} \\
t &= \frac{DRAM\_traffic}{peak\_DRAM\_BW} \\
&= \frac{B \times T \times (\text{sum of all above})}{peak\_DRAM\_BW}.
\end{aligned}$$

The subscript  $w$  denotes that these are per-WARP DRAM traffic; the value  $B \times T$  is the total number of WARPs. For the backward kernel, we simply replace the per-WARP weights traffic by

$$tr\_weights_w = \lceil 2 \times 4 \times L \times D/32 \rceil \times 32 \text{ bytes},$$

and follow exactly the same other equations.

This method can be further enhanced by estimating the L2 cache hit rate of accessing the embedding lookup table and separating the total memory traffic into DRAM traffic and L2 traffic. As one thread WARP is responsible for computing one vector in the output tensor, assuming only one CTA resides on each streaming-multiprocessor (SM) on the GPU at a time, the number of embedding lookup tables whose (at least part of) data simultaneously reside in L2 cache is given by

$$num\_tables = rows\_per\_block \times (\#SM)/B,$$

where  $rows\_per\_block$  is an argument of the kernel that specifies how many output vectors are computed per CTA. With the L2 cache size of the GPU known to us, we can calculate the number of rows per table that resides in the L2 cache as

$$avg\_cached\_rows\_per\_table = \min\left(\frac{L2\_cache\_size}{(num\_tables) \times D}, E\right),$$

where the second term covers the case when an embedding lookup table with  $E$  rows has a size small enough to stay in the L2 cache all the time. Therefore, the hit rate of the L2 cache, i.e., the probability that the accesses to a total of  $L$  embedding lookup table row vectors among all  $E$  vectors, can be estimated by

$$p = \frac{\binom{avg\_cached\_rows\_per\_table}{L}}{\binom{E}{L}}.$$

Notice that the  $table\_offsets$  and  $offsets$  tensors are relatively small and thus we assume they always stay in L2. Therefore, we construct the enhanced performance model as:

$$\begin{aligned}
tr_{L2} &= tr\_table\_offsets_w + tr\_offsets_w + p \times tr\_weights_w \\
tr_{DRAM} &= tr\_indices_w + tr\_outputs_w + (1 - p) \times tr\_weights_w \\
t &= \frac{DRAM\_traffic}{peak\_DRAM\_BW} + \frac{L2\_traffic}{peak\_L2\_BW} \\
&= B \times T \times \left( \frac{tr_{DRAM}}{peak\_DRAM\_BW} + \frac{tr_{L2}}{peak\_L2\_BW} \right).
\end{aligned}$$

2) *Characterizing GEMM Kernels:* We take  $batch\_size$ ,  $M$ ,  $N$ , and  $K$  of a batched GEMM operation as the input feature of the MLP model to predict the kernel execution time as the only output feature. We conduct a grid search for the best configuration. The search space is shown in Table II and the loss function is Mean Square Error (MSE). As the input sizes of the benchmark are chosen in an almost exponential scale, e.g., 32, 64, 128, etc, we preprocess the dataset by taking logarithm values of both the sizes and the results. We also scale the learning rate by 10 if *SGD* is chosen as the optimizer.

TABLE II. MLP performance model search space.

Hyperparameter	Range
num_layers	[3,4,5,6,7]
num_neurons_per_layer	[128,256,512,1024]
optimizer	[Adam, SGD]
learning_rate	[1e-4, 2e-4, 5e-4, 1e-3, 2e-3, 5e-3, 1e-2]

3) *Characterizing Memory and Element-wise Kernels:* For memory kernels of ops including *concat*, *memcpy*, etc., as well as element-wise kernels of ops like *ReLU*, *sigmoid*, etc., it is straightforward to estimate their execution time by applying the roofline model [12]:

$$\begin{aligned}
t &= \max(t\_compute, t\_memory) \\
&= \max\left(\frac{FLOP}{peak\_throughput}, \frac{bytes_{read} + bytes_{write}}{peak\_BW}\right).
\end{aligned}$$

We use the maximum measured bandwidth of the benchmark as the corrected peak bandwidth in calculation. Specifically, we find that it is non-trivial to model the performance of transpose ops like *T* or *permute*, because technically the underlying implementations of tensor transpose might differ significantly, yet these implementations are opaque to users in PyTorch since the kernel is JIT-generated. Therefore, we adopt the ML performance modeling approach by training an MLP with the same search space as that of the GEMM kernels.

### C. Device Idle Time Analysis

Device idle time, as we show in Figure 5, is an important part of the total device execution time. We predict device idle time based on overheads obtained by analyzing the trace files generated by profilers. In a single-GPU context, the main source of device idle time is the *host overheads that are not hidden*. There are two assumptions we make for these overheads:

- **Model-independence:** Same types of overheads of the same op have the same stats on the same machine.

- Size-independence: Overheads do not depend on input/output tensor sizes of ops.

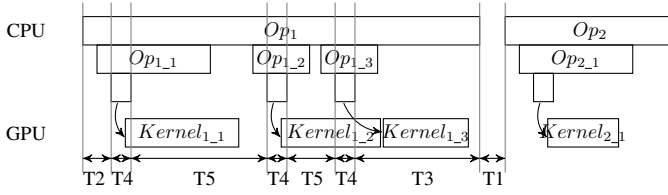


Fig. 7. Host-side overhead types. The labels T1–T5 indicate the five overhead types introduced in Section III-C. Each op has one T2 and one T3 overhead, and at least one T4 overhead if it has device kernel calls.

That means overheads are supposed to be only dependent to the training platform (i.e., CPUs) configurations. Based on these two assumptions, we analyze the host-side overheads and categorize them into five types as shown in Figure 7, including:

- Type 1: Overhead between two top-level PyTorch op calls.
- Type 2: Overhead before an op’s first kernel launch begins.
- Type 3: Overhead after an op’s last kernel launch ends.
- Type 4: Execution time of CUDA runtime functions, e.g., `cudaLaunchKernel`, `cudaMemcpyAsync`, etc.
- Type 5: Overheads between two kernel launches.

Some of the overheads, namely T2, T3, and T5, should be independent of the input parameters of the op, as we assume all the parameter-defined operations, mainly the computation and data movements, are offloaded to the device. By analyzing 100-iteration trace files of the models we choose, we characterize each type of overheads and store their mean values in a JSON file that will be used in the end-to-end performance model. In the meantime, profiler overheads of CPU and GPU events are subtracted from these overheads to guarantee the accuracy of them. In practice we use  $4 \mu s$  as indicated in the PyTorch source code to model the profiler overheads of GPU events, while that of CPU events vary from platform to platform, and we find that an empirical value of  $2 \mu s$  is a good choice.

#### D. End-to-end GPU Training Performance Model

One challenge of building an end to end performance model of an ML training workload is to have sufficient information about its run-time execution. Early implementations of ML frameworks such as Caffe [30] define an ML model as a static graph in the protobuf format. In recent years, ML frameworks such as TensorFlow [31] and PyTorch [32] have closely integrated programming language bindings to support dynamic ML model graphs characterized by conditionals and loops. Furthermore, they support eager mode execution. With the flexibility of these frameworks, the ML model definition is essentially a program and requires execution to fully capture the run-time characteristics. We implemented an execution graph observer inside PyTorch that allows us to extract both the operators executed and their inputs and outputs data dependencies during the model training process. Once the ML model’s run-time execution is captured, the execution graph can be reconfigured to use different data inputs or hardware devices. For example, we may collect the execution graph while running on CPU and apply our performance models to

the execution graph to predict the workload’s performance on the GPU or other types of hardware.

#### Algorithm 1 End-to-end GPU Training Performance Model.

```

1: Input: Execution graph  $G$  of a DLRM model; Kernel
   performance models  $\{M\}$ ; Overheads  $ov$ .
2: Output: Predicted per-batch training time  $T$ .
3: Initialize  $cpu\_time = 0, gpu\_time = 0$ 
4: for each  $op$  in  $G$  do
5:   Look up  $T1, T2, T3, T4, T5$  from  $ov$  for  $op$ 
6:    $cpu\_time += T1$ 
7:   if  $op$  has kernel calls then
8:      $cpu\_time += T2$ 
9:     for each kernel  $k$   $op$  calls do
10:      Predict kernel time  $T_k$  with the corresponding
        performance model picked from  $\{M\}$ 
11:       $gpu\_time = \max(gpu\_time + 1, cpu\_time +$ 
         $T4/2) + T_k$ 
12:       $cpu\_time += T4$ 
13:      if  $k$  is not the last kernel then
14:         $cpu\_time += T5$ 
15:      end if
16:    end for
17:     $cpu\_time += T3$ 
18:   else
19:      $cpu\_time += T5$ 
20:   end if
21: end for
22:  $T = \max(gpu\_time, cpu\_time)$ 

```

We devise a critical-path-based Algorithm 1 that integrates the predicted kernel time and overheads to predict the end-to-end training time of DLRM. We keep track of both the execution time on CPU and GPU. For each operator, we first add T1 and T2 to the CPU time as a prerequisite. If the op has kernel calls, we set the start time of each kernel based on whether the CPU or GPU time is the critical path (line 11), so that the device idle time caused by the host overheads is counted. Each kernel time is then added to the GPU time, while T4 and T5 are added to the CPU time. T3 is added after all kernels are processed. Eventually, we take the maximum of CPU and GPU time as the final end-to-end predicted time.

#### IV. RESULTS AND ANALYSIS

We evaluate our benchmark and performance models on three different NVIDIA GPUs—Tesla V100, Tesla P100, and GeForce GTX TITAN Xp—with CUDA 11.3 and Python 3.9. We conduct the end-to-end tests on three open-sourced DLRM models that can be accessed in Facebook’s DLRM repo on Github [33]. We name them DLRM\_default, DLRM\_MLPerf, and DLRM\_DDP. To launch the training of the DLRM\_MLPerf model, we use the Kaggle Criteo dataset as the training dataset, and change the embedding table sparse feature size of *DLRM\_MLPerf* from 128 to 32 to allow it to fit into the memory of TITAN Xp and P100. We also use the code repository of Konstantinidis et al. [35] to benchmark the GPU hardware

TABLE III. Execution time prediction error for each of the dominating kernels. Abbreviation examples: **EL** (embedding lookup), **GEMM** (fully connected and interaction layers), **memcpy** (memory copy from host to device), **concat** (concatenation), **tril** (lower triangular extraction and flatten), **F** (forward), **B** (backward), **H** (with hit rate estimation for EL), **L** (large size, average embedding table size greater than 100000).

GPU Kernel	GMAE	V100 mean	std	GMAE	TITAN Xp mean	std	GMAE	P100 mean	std
EL-F	11.46%	35.92%	56.81%	12.81%	34.05%	38.92%	8.63%	33.19%	54.72%
EL-FL	6.93%	11.22%	8.96%	7.54%	16.76%	16.01%	2.89%	5.52%	6.26%
EL-FH	9.27%	16.73%	16.39%	11.88%	25.44%	26.04%	6.42%	13.06%	14.81%
EL-FHL	7.85%	12.68%	10.02%	8.84%	18.20%	16.68%	3.84%	7.02%	7.08%
EL-B	9.53%	34.39%	60.91%	8.31%	38.62%	65.77%	12.49%	35.26%	62.70%
EL-BL	5.27%	5.94%	2.29%	2.38%	2.95%	1.61%	9.88%	10.13%	2.37%
EL-BH	7.39%	13.37%	15.01%	5.57%	15.16%	23.99%	8.42%	12.59%	12.12%
EL-BHL	5.69%	6.24%	2.28%	2.55%	3.21%	1.68%	10.19%	10.42%	2.33%
GEMM	5.80%	10.00%	10.33%	8.92%	14.24%	11.83%	7.59%	12.30%	10.39%
concat	5.34%	11.45%	14.76%	8.17%	11.48%	9.08%	3.30%	6.54%	12.63%
memcpy	0.57%	0.96%	2.46%	7.05%	13.87%	17.45%	5.10%	7.95%	8.28%
transpose	2.95%	5.47%	6.71%	5.75%	10.13%	9.67%	3.35%	5.92%	6.84%
tril-F	2.13%	3.67%	3.81%	3.23%	6.54%	8.17%	3.71%	6.74%	8.31%
tril-B	3.67%	7.35%	9.40%	3.08%	6.69%	9.30%	2.71%	4.76%	4.51%

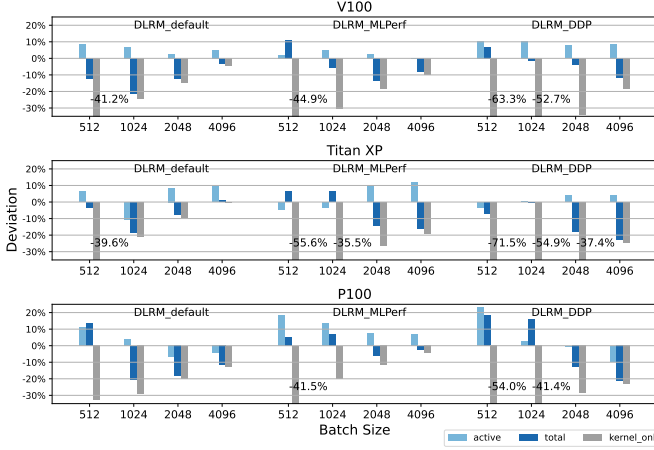


Fig. 8. End-to-end per-batch training time prediction of three DLRM models on three different devices. *active*, *total*, *kernel\_only* are respectively the prediction errors of GPU active time, end-to-end per-batch time, and using sum of predicted kernel time as the end-to-end time without device idle time modeling. parameters, e.g., FLOPS, DRAM bandwidth, etc. that are needed by the heuristic performance models.

#### A. Performance Models for Dominating Kernels in DLRM

In Table III we can see that on all types of GPU, our plain performance model for batched embedding table lookup achieves a varying yet low error rate for all table sizes and a stable and lower error rate for big table sizes ( $E > 100k$ ). This is because when the lookup tables are small, the L2 cache can capture substantial locality, and thus our assumption that lookup traffic comes from DRAM is no longer valid. However, with our enhanced performance model, we successfully reduce and stabilize the error rate for all table sizes while still maintaining a lower error rate for big table sizes. Thus we adopt the enhanced model in our end-to-end analysis. Except for embedding lookup, we also achieve decent (i.e., less than 10%) GMAE errors on both ML-based models and other heuristic models for all other kernels. The errors of our kernel performance models correlate across all three different GPU devices.

#### B. End-to-end GPU Training Performance Model for DLRM and More DL Models

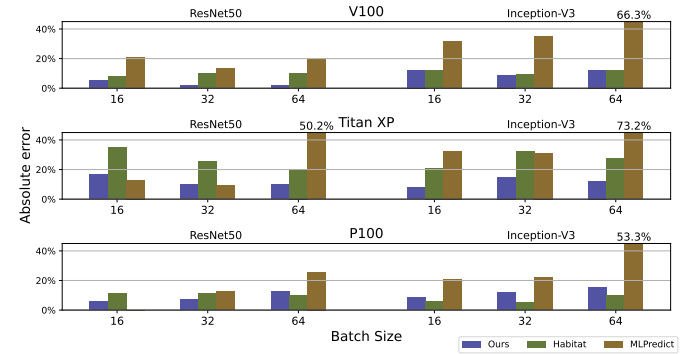


Fig. 9. End-to-end per-batch training time prediction of ResNet50 and Inception-V3 as representatives of non-DLRM DL models on three different GPUs. We used Habitat open source project to collect the prediction result on TITAN Xp since it was not reported in the paper.

We evaluate our end-to-end prediction on the three DLRM models on our three GPUs and show the results in Table IV and Figure 8. We predict the device active time by summing up the execution time of relevant kernels, and also the end-to-end training time with our proposed algorithm. We see that the geomean values of active time and end-to-end time prediction error are 5.23% and 7.96%, respectively. Notice the *kernel\_only* prediction errors are much worse than *total*, which justifies the necessity and success of including the modeling of device idle time in our prediction algorithm. Device-wise, the GPU active time error on V100 is the lowest among the three, while the end-to-end error is the lowest on the platform with TITAN Xp. The prediction error of the device active time comes from the kernel execution time prediction error. For example, the MLPerf model has non-constant table sizes and thus we have to use the average table size in the performance model, which affects its accuracy. Overall, the device active time error rate lies within the range of our expectation, which is a proof of



TABLE IV. Statistics of active (kernel) time and end-to-end time prediction errors across three platforms.

	Overall			V100			TITAN Xp			P100		
	geomean	min	max	geomean	min	max	geomean	min	max	geomean	min	max
Active	<b>5.23%</b>	0.38%	23.53%	4.50%	0.45%	10.63%	5.06%	0.56%	12.07%	6.29%	0.38%	23.53%
E2E	<b>7.96%</b>	0.53%	22.75%	7.49%	1.32%	21.48%	6.33%	0.53%	22.75%	10.64%	2.20%	21.20%

success of the kernel performance model. Compared to the active time predictions that usually tend to be overestimated (26 out of 36 cases), the end-to-end time predictions, however, has a reverse trend of underestimation (25 of 36 cases), which can be explained by the underestimation of device idle time. We suspect that it is because some of the overheads, e.g., T1, or T4 of *cudaMemcpyAsync*, etc, have long-tail distribution with high variation, while we use their mean values in the predictions. Since these are usually popular overheads (T1 is the most popular one as it comes with every single op), the error might accumulate quickly and thus results in underestimation of device idle time and end-to-end time. In addition, we observe no systematic or correlated errors in either active or idle time and are confident that the end-to-end device active time and total time are appropriately predicted.

As Figure 9 shows, we also compare our performance model on two CV models, i.e., ResNet50 and Inception-V3, with two previous works, *Habitat* [16] and *MLPredict* [17], neither of which supports DLRM mainly because of the limited coverage of ops. We do not compare with *Daydream* as it is not open-source and does not make end-to-end predictions. To enable the prediction of these two models, we extend our microbenchmark to cover the convolution and batch-normalization ops. We can see that our work achieves comparable or better prediction errors against the two previous works. The reason *MLPredict* fails to produce accurate results on some of the tests might be that the predictor they trained does not cover certain batch sizes (possibly due to GPU memory limits) and/or certain convolution input sizes (such as Inception-V3’s  $1 \times 7$  and  $7 \times 1$  convolution filters).

### C. Discussion: Performance Modeling for Model-System Co-design

How can our performance model assist further optimization? The advantages of our performance model against previous works are: (1) we are able to more accurately predict individual kernel performance and op overheads and (2) our execution graph captures data dependencies between ops. Therefore, we are able to provide more comprehensive and flexible simulation and performance modeling options than both previous works and trace file inspection. Typical use cases include iterative model tuning and op optimization such as fusion.

*a) Iterative Model Tuning:* To ensure both high precision/recall and fast training speed, the iterative tuning of configurations of ML models (e.g., number of bottom/top MLP layers and neurons per layer, and the number of embedding tables in DLRM) is necessary yet might be difficult, especially when frequently launching training trials for the ML models in an industrial environment is costly and not always practical. With our performance model, users can handily

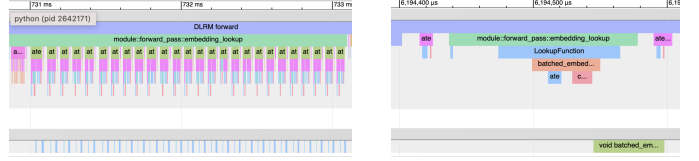


Fig. 10. Separate embedding bag ops (left) and batched embedding op (right).

make transformations like *insert*, *remove*, *replace*, *resize*, and *parallelize* on our easily mutable execution graph and predict the outcome of their optimization without actually running the code. Specifically, it is straightforward to change metadata of tensor shapes of selected ops and their parent and child nodes in the graph for *resize*, and to assign ops in parallel branches with no data dependency to different GPU streams for *parallel*. This can only be performed with the support of data dependencies between ops and individual kernel runtime prediction in our performance model. In fact, our performance model could potentially be integrated as a module into network architecture search (NAS) and significantly improve automatic search for the best ML model configuration. We see this as exciting future work.

*b) Op Fusion:* Op fusion is a common optimization technique that brings speedup by replacing multiple ops with a mathematically equivalent one. When users implement a new op, it is good to know how it improves the performance in a ML model generally (i.e., with arbitrary input tensor shapes). Figure 10 shows an example of optimization that we have done with the performance model. On the left side it shows a series of embedding bag ops as a good target (i.e., causing too much device overheads) to be optimized by fusing them into a batched embedding op, as shown in the right side. We easily modify the execution graph and replace the subgraph of all embedding bag ops with arbitrary input shapes with one single batched embedding op, whose performance is then predicted by the kernel performance model we design. This is extremely efficient when there are a large number of ML models to be optimized and evaluated, since we never need to launch jobs and benchmark them.

*c) Load Balancing:* In the cases of multi-GPU training, subgraphs that are too expensive to be computed on one single device are distributed to several through data- or model-parallelism. This is also a common practice for DLRM, especially the enormous embedding tables. Our performance model enables the evaluation of each device’s performance upon any schemes of splitting embedding tables that results in different combinations of embedding table sizes on these devices. Again, this greatly accelerates the development and debugging of DLRM training on multi-GPU platforms.

## V. CONCLUSION AND FUTURE WORK

We propose a performance model for GPU training of DLRM as well as other ML models. Our model is a more general methodology than simply predicting the end-to-end time as the sum of kernel time, which does not work well in models with low GPU utilization. Future work includes investigating performance modeling of communication collectives (e.g., *all\_to\_all*, *all\_reduce*) so as to model of DLRM training on multi-node multi-GPU platforms. Another of our goals is to model the performance of embedding lookups with a non-constant number of embeddings and number of lookups per table, which should improve our overall model accuracy. Finally, we would also love to develop a tool that visualizes and facilitates the manipulation of execution graphs for model-system co-design.

## REFERENCES

- [1] M. Tennenholtz and O. Kurland, "Rethinking search engines and recommendation systems: A game theoretic perspective," *Commun. ACM*, vol. 62, no. 12, pp. 66–75, Nov. 2019. [Online]. Available: <https://doi.org/10.1145/3340922>
- [2] B. Smith and G. Linden, "Two decades of recommender systems at Amazon.com," *IEEE Internet Computing*, vol. 21, no. 03, pp. 12–18, May/Jun. 2017.
- [3] P. Covington, J. Adams, and E. Sargin, "Deep neural networks for YouTube recommendations," in *Proceedings of the 10th ACM Conference on Recommender Systems*, ser. RecSys '16, 2016, pp. 191–198. [Online]. Available: <https://doi.org/10.1145/2959100.2959190>
- [4] E. Elahi and A. Chandrashekar, "Learning representations of hierarchical slates in collaborative filtering," in *Fourteenth ACM Conference on Recommender Systems*, ser. RecSys '20, 2020, pp. 703–707. [Online]. Available: <https://doi.org/10.1145/3383313.3418484>
- [5] Q. Song, D. Cheng, H. Zhou, J. Yang, Y. Tian, and X. Hu, "Towards automated neural interaction discovery for click-through rate prediction," in *Proceedings of the 26th ACM SIGKDD International Conference on Knowledge Discovery & Data Mining*, ser. KDD '20, 2020, pp. 945–955. [Online]. Available: <https://doi.org/10.1145/3394486.3403137>
- [6] W. Zhao, J. Zhang, D. Xie, Y. Qian, R. Jia, and P. Li, "Aibox: Ctr prediction model training on a single node," in *Proceedings of the 28th ACM International Conference on Information and Knowledge Management*, ser. CIKM '19, 2019, pp. 319–328.
- [7] W. Zhao, D. Xie, R. Jia, Y. Qian, R. Ding, M. Sun, and P. Li, "Distributed hierarchical GPU parameter server for massive scale deep learning ads systems," in *Proceedings of Machine Learning and Systems 2020*, ser. MLSys 2020, I. S. Dhillon, D. S. Papailiopoulos, and V. Sze, Eds. mlsys.org, Mar. 2020. [Online]. Available: <https://proceedings.mlsys.org/book/315.pdf>
- [8] M. Naumov, D. Mudigere, H. M. Shi, J. Huang, N. Sundaraman, J. Park, X. Wang, U. Gupta, C. Wu, A. G. Azzolini, D. Dzhulgakov, A. Mallevich, I. Cherniavskii, Y. Lu, R. Krishnamoorthi, A. Yu, V. Kondratenko, S. Pereira, X. Chen, W. Chen, V. Rao, B. Jia, L. Xiong, and M. Smelyanskiy, "Deep learning recommendation model for personalization and recommendation systems," *CoRR*, vol. abs/1906.00091, 2019. [Online]. Available: <https://arxiv.org/abs/1906.00091>
- [9] P. Mattson, C. Cheng, G. Diamos, C. Coleman, P. Micikevicius, D. Patterson, H. Tang, G.-Y. Wei, P. Bailis, V. Bittorf, D. Brooks, D. Chen, D. Dutta, U. Gupta, K. Hazelwood, A. Hock, X. Huang, D. Kang, D. Kanter, N. Kumar, J. Liao, D. Narayanan, T. Oguntebi, G. Pekhimenko, L. Pentecost, V. Janapa Reddi, T. Robie, T. St John, C.-J. Wu, L. Xu, C. Young, and M. Zaharia, "Mlperf training benchmark," in *Proceedings of Machine Learning and Systems*, I. Dhillon, D. Papailiopoulos, and V. Sze, Eds., vol. 2, 2020, pp. 336–349. [Online]. Available: <https://proceedings.mlsys.org/paper/2020/file/02522a2b2726fb0a03bb19f2d8d9524d-Paper.pdf>
- [10] K. He, X. Zhang, S. Ren, and J. Sun, "Deep residual learning for image recognition," in *2016 IEEE Conference on Computer Vision and Pattern Recognition (CVPR)*, 2016, pp. 770–778.
- [11] A. Vaswani, N. Shazeer, N. Parmar, J. Uszkoreit, L. Jones, A. N. Gomez, L. u. Kaiser, and I. Polosukhin, "Attention is all you need," in *Advances in Neural Information Processing Systems*, I. Guyon, U. V. Luxburg, S. Bengio, H. Wallach, R. Fergus, S. Vishwanathan, and R. Garnett, Eds., vol. 30. Curran Associates, Inc., 2017.
- [12] S. Williams, A. Waterman, and D. Patterson, "Roofline: An insightful visual performance model for multicore architectures," *Communications of the ACM*, vol. 52, no. 4, pp. 65–76, 2009.
- [13] NVIDIA. (2020, Jul.) cuBLAS deep learning performance matrix multiplication. [Online]. Available: <https://docs.nvidia.com/deeplearning/performance/dl-performance-matrix-multiplication/index.html>
- [14] S. Lym, D. Lee, M. O'Connor, N. Chatterjee, and M. Erez, "DeLTA: GPU performance model for deep learning applications with in-depth memory system traffic analysis," in *2019 IEEE International Symposium on Performance Analysis of Systems and Software (ISPASS)*, Mar. 2019, pp. 293–303.
- [15] Y.-C. Liao, C.-C. Wang, C.-H. Tu, M.-C. Kao, W.-Y. Liang, and S.-H. Hung, "Perfnetr: Platform-aware performance modeling for optimized deep neural networks," in *2020 International Computer Symposium*, ser. ICS 2020, 2020, pp. 153–158.
- [16] G. X. Yu, Y. Gao, P. A. Golikov, and G. Pekhimenko, "Computational performance predictions for deep neural network training: A runtime-based approach," *CoRR*, vol. abs/2102.00527, 2021. [Online]. Available: <https://arxiv.org/abs/2102.00527>
- [17] D. Justus, J. Brennan, S. Bonner, and A. McGough, "Predicting the computational cost of deep learning models," Dec. 2018, pp. 3873–3882.
- [18] Z. Pei, C. Li, X. Qin, X. Chen, and G. Wei, "Iteration time prediction for CNN in multi-GPU platform: Modeling and analysis," *IEEE Access*, vol. 7, pp. 64 788–64 797, 2019.
- [19] S. Li, R. J. Walls, and T. Guo, "Characterizing and modeling distributed training with transient cloud GPU servers," in *2020 IEEE 40th International Conference on Distributed Computing Systems (ICDCS)*, 2020, pp. 943–953.
- [20] H. Zhu, A. Phanishayee, and G. Pekhimenko, "Daydream: Accurately estimating the efficacy of optimizations for DNN training," in *2020 USENIX Annual Technical Conference, USENIX ATC 2020, July 15-17, 2020*, A. Gavrilovska and E. Zadok, Eds. USENIX Association, 2020, pp. 337–352.
- [21] J. L. Herlocker, J. A. Konstan, and J. Riedl, "Explaining collaborative filtering recommendations," in *Proceedings of the 2000 ACM Conference on Computer Supported Cooperative Work*, ser. CSCW '00, 2000, pp. 241–250. [Online]. Available: <https://doi.org/10.1145/358916.358995>
- [22] X. Ning, C. Desrosiers, and G. Karypis, "A comprehensive survey of neighborhood-based recommendation methods," in *Recommender Systems Handbook*, F. Ricci, L. Rokach, and B. Shapira, Eds. Springer, 2015, pp. 37–76. [Online]. Available: [https://doi.org/10.1007/978-1-4899-7637-6\\_2](https://doi.org/10.1007/978-1-4899-7637-6_2)
- [23] S. H. Walker and D. B. Duncan, "Estimation of the probability of an event as a function of several independent variables," *Biometrika*, vol. 54, no. 1–2, pp. 167–179, Jun. 1967.
- [24] H. Guo, R. Tang, Y. Ye, Z. Li, and X. He, "DeepFM: A factorization-machine based neural network for CTR prediction," in *Proceedings of the 26th International Joint Conference on Artificial Intelligence*, ser. IJCAI'17. AAAI Press, 2017, pp. 1725–1731.
- [25] H.-T. Cheng, L. Koc, J. Harmsen, T. Shaked, T. Chandra, H. Aradhye, G. Anderson, G. Corrado, W. Chai, M. Ispir, R. Anil, Z. Haque, L. Hong, V. Jain, X. Liu, and H. Shah, "Wide & deep learning for recommender systems," in *Proceedings of the 1st Workshop on Deep Learning for Recommender Systems*, ser. DLRS 2016, 2016, pp. 7–10. [Online]. Available: <https://doi.org/10.1145/2988450.2988454>
- [26] J. Lian, X. Zhou, F. Zhang, Z. Chen, X. Xie, and G. Sun, "XDeepFM: Combining explicit and implicit feature interactions for recommender systems," in *Proceedings of the 24th ACM SIGKDD International Conference on Knowledge Discovery & Data Mining*, ser. KDD '18, 2018, pp. 1754–1763. [Online]. Available: <https://doi.org/10.1145/3219819.3220023>
- [27] R. Wang, B. Fu, G. Fu, and M. Wang, "Deep & cross network for ad click predictions," in *Proceedings of the ADKDD'17*, ser. ADKDD'17, 2017. [Online]. Available: <https://doi.org/10.1145/3124749.3124754>
- [28] G. Zhou, X. Zhu, C. Song, Y. Fan, H. Zhu, X. Ma, Y. Yan, J. Jin, H. Li, and K. Gai, "Deep interest network for click-through rate prediction," in *Proceedings of the 24th ACM SIGKDD International Conference on Knowledge Discovery & Data Mining*, ser. KDD '18, 2018, pp. 1059–1068. [Online]. Available: <https://doi.org/10.1145/3219819.3219823>

- [29] A. Tulloch. (2020, May) Batch embedding lookup GPU kernel and more. [Online]. Available: <https://github.com/ajtulloch/sparse-ads-baselines>
- [30] Y. Jia, E. Shelhamer, J. Donahue, S. Karayev, J. Long, R. Girshick, S. Guadarrama, and T. Darrell, "Caffe: Convolutional architecture for fast feature embedding," in *Proceedings of the 22nd ACM International Conference on Multimedia*, ser. MM '14, 2014, pp. 675–678.
- [31] M. Abadi, P. Barham, J. Chen, Z. Chen, A. Davis, J. Dean, M. Devin, S. Ghemawat, G. Irving, M. Isard, M. Kudlur, J. Levenberg, R. Monga, S. Moore, D. G. Murray, B. Steiner, P. Tucker, V. Vasudevan, P. Warden, M. Wicke, Y. Yu, and X. Zheng, "Tensorflow: A system for large-scale machine learning," in *12th USENIX Symposium on Operating Systems Design and Implementation (OSDI 16)*, 2016, pp. 265–283. [Online]. Available: <https://www.usenix.org/system/files/conference/osdi16/osdi16-abadi.pdf>
- [32] A. Paszke, S. Gross, F. Massa, A. Lerer, J. Bradbury, G. Chanan, T. Killeen, Z. Lin, N. Gimelshein, L. Antiga, A. Desmaison, A. Köpf, E. Yang, Z. DeVito, M. Raison, A. Tejani, S. Chilamkurthy, B. Steiner, L. Fang, J. Bai, and S. Chintala, "Pytorch: An imperative style, high-performance deep learning library," in *Advances in Neural Information Processing Systems 32*, ser. NeurIPS 2019, 2019.
- [33] Facebook. (2019, Jun.) DLRM Github repo. [Online]. Available: <https://github.com/facebookresearch/dlrm>
- [34] D. Kalamkar, E. Georganas, S. Srinivasan, J. Chen, M. Shiryayev, and A. Heinecke, "Optimizing deep learning recommender systems training on CPU cluster architectures," in *Proceedings of the International Conference for High Performance Computing, Networking, Storage and Analysis*, ser. SC '20, Nov. 2020, pp. 1–15.
- [35] E. Konstantinidis and Y. Cotronis, "A quantitative roofline model for GPU kernel performance estimation using micro-benchmarks and hardware metric profiling," *Journal of Parallel and Distributed Computing*, vol. 107, pp. 37–56, 2017. [Online]. Available: <https://www.sciencedirect.com/science/article/pii/S0743731517301247>